Basin Modeling: Pressure Prediction for the Marine Jequitinhonha

Lourenildo W. B. Leite, Wildney W. S. Vieira and Aucilene N. P. da Silva, UFPA, Brazil

Abstract

This paper aims at the composition of a seismic-stratigraphical framework for part of Jequitinhonha basin (marine east part of the State of Bahia), for pressure prediction in gas and oil exploration in sedimentary basins. The knowledge of the velocity distributions can be based on seismic sections, petrophysical information and empirical model, and it is based on the knowledge of the compressional (v_P) and shear (v_S) velocities, and densities (ρ). We presented details of the theoretical model, and an example to show how the pressure varies in the subsurface, where we highlight that pressure prediction does not necessarily increase linearly, but in a complex way that requires specific numerical formulas to be able to see important details. The model poses the vertical gravity load as pressure agent on the geological formations, and does not take into account the effects of curvatures, faulting and diagenesis, and lateral tectonic events. An accurate prediction needs a 3D model for a significantly complete practical application.

INTRODUCTION

This paper is a numerical experiment, and for the present case four seismic lines were used and separated into two groups, three lines in the NE-SW (L214-266, L214-268, L214-270) and one in the NW-SE direction (L214-297).

The methodology was composed of velocity analysis, CRS stacking, CRS migration, interpretation, and construction of a controlled empirical model for P and S wave velocities and density, culminating in the prediction of subsurface pressure, which aims at mapping areas of low (example, rock reservoir) and high (example, rock generator) pressure zones acting as natural pumps for the accumulation of fluids (Payton, 1977; Mann, 2002; Cohen and Stockwell, 2005).

The principle of seismic interpretation is to recognize the textures existing between the main reflective patterns, where 4 basic principles were considered: resolution (vertical), continuity (horizontal), texture (of the intervals between dominant events), and frequency content (low, medium, high).

The Regência Petroleum System is responsible for all hydrocarbon occurrences in the Jequitinhonha Basin. However, it is necessary to emphasize that a rock is a reservoir candidate if it fulfills the mechanical-static conditions of pressure (Mello et al., 1994; Sibiryakov et al., 2014; Silva, 2016).

METHODOLOGY

Figures 1 show the interpreted sections over the CRS zero offset stacked, based on reflections with lateral continuity of the reflector, and texture of the macro segments, and where the sequences and structures are indicated by letters and numbers.

Figure 1: Seismic interpretation.

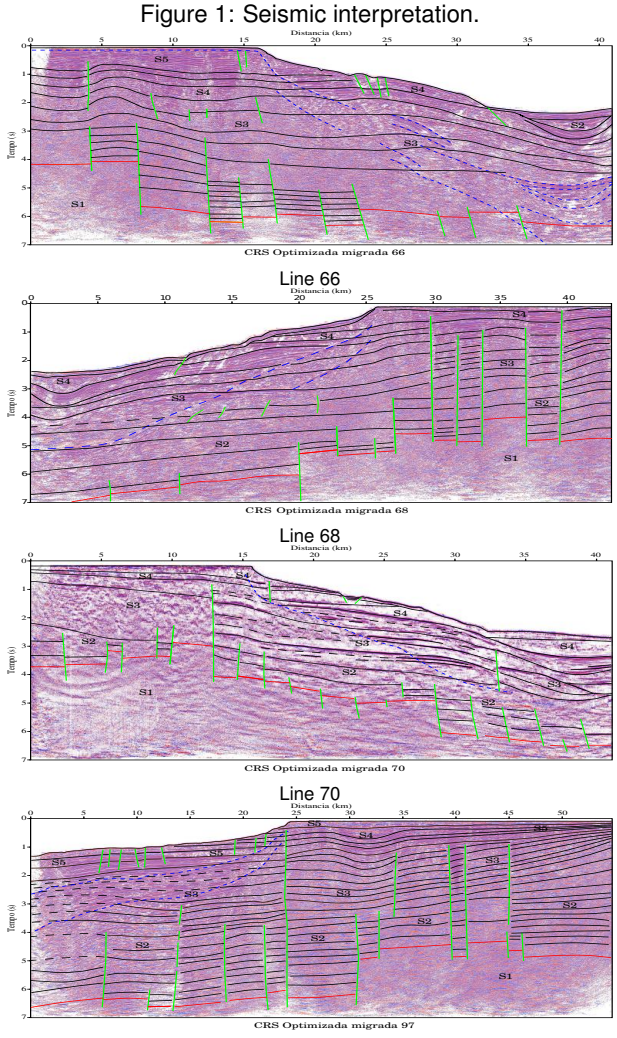

Pressure Prediction

The main physical parameter governing this phenomenon is the measure of discontinuity represented by the ratio $\gamma =$

v_S/v_P along the interfaces. As a result of these studies, (Sibiryakov et al., 2015) is an example dealing with different aspects of research topic.

As a result of the γ ratio behavior, an anticline is not necessarily the only structural condition for potentiating a zone to be a oil and gas accumulator.

The continuous linear elastic stress fields, $\sigma = \sigma(x,y,z)$, and deformation, $\varepsilon = \varepsilon(x,y,z)$, are related by Hooke's Law, described as tensors, functions of space, and which are represented by nine components. For the general anisotropic media, the tensors (σ) and (ε) obey the spatial coordinate rotation by the relation: $\sigma_{ij} = \sum_{k,l} a_{jkl}\sigma'_{kl}$, and $\varepsilon_{ij} = \sum_{k,l} b_{jjkl}\varepsilon'_{kl}$, where the coefficients a_{ijkl} and b_{ijkl} define the new plane with respect to a reference system. The elastic linear relationship between stress and strain is given by the generalized Hooke's law: $\sigma_{ij} = \sum_{k,} c_{ijkl}\varepsilon_{kl}$. In this description, the first index (i) in σ_{ij} and in ε_{jj} represents the plane direction, and the second (j) the component direction. The stress state is represented at a point Q by a matrix $\mathbf{S}$ with elements σ_{ij}. The differential equations serve to represent a physical particle of the subsurface, and the seek solution is the integration of these infinitesimal quantities that result in the desired formulas.

Stress states

The stress matrix can be decomposed into three parts in the form: $\mathbf{S} = \mathbf{S_0} + \mathbf{S_D}\mathbf{S_N}$, which allows a physical interpretation (Persen, 1975). For the state $\mathbf{S_0}$ one has simply $\mathbf{S_0} = \{P_H\delta_{ij}\}$ where $P_H = \frac{1}{3}(\sigma_{xx} + \sigma_{yy} + \sigma_{zz})$ is the sum of the normal stresses which define the so-called hydrostatic pressure, and this state is present in any plane around the point Q. For the state $\mathbf{S_D}$ one has that:

$$\mathbf{S_D} = \begin{bmatrix} \sigma_{xx} - P_H & \frac{1}{2}(\sigma_{xy} + \sigma_{yx}) & \frac{1}{2}(\sigma_{xz} + \sigma_{zx}) \\ \frac{1}{2}(\sigma_{xy} + \sigma_{yx}) & \sigma_{yy} - P_H & \frac{1}{2}(\sigma_{yz} + \sigma_{zy}) \\ \frac{1}{2}(\sigma_{xz} + \sigma_{zx}) & \frac{1}{2}(\sigma_{zy} + \sigma_{yz}) & \sigma_{zz} - P_H \end{bmatrix}. \quad (1)$$

Applying the symmetry property to the above matrix (1): $\sigma_{xy} = \sigma_{yx}$, $\sigma_{xz} = \sigma_{zx}$, $\sigma_{yz} = \sigma_{zy}$, $\mathbf{S_D}$, results in a null state, i. e., $\mathbf{S_D} = \mathbf{0}$. For the state $\mathbf{S_N}$:

$$\mathbf{S_N} = \begin{bmatrix} 0 & \frac{1}{2}(\sigma_{xy} - \sigma_{yx}) & \frac{1}{2}(\sigma_{xz} - \sigma_{zx}) \\ \frac{1}{2}(\sigma_{xy} - \sigma_{yx}) & 0 & \frac{1}{2}(\sigma_{yz} - \sigma_{zy}) \\ \frac{1}{2}(\sigma_{xz} - \sigma_{zx}) & \frac{1}{2}(\sigma_{zy} - \sigma_{yz}) & 0 \end{bmatrix}. \quad (2)$$

In the same form, applying the symmetry property, the state $\mathbf{S_N}$ simplifies to:

$$\mathbf{S_N} = \begin{bmatrix} \sigma_{xx} - P_H & \sigma_{xy} & \sigma_{xz} \\ \sigma_{yx} & \sigma_{yy} - P_H & \sigma_{xz} \\ \sigma_{zx} & \sigma_{zx} & \sigma_{zz} - P_H \end{bmatrix}. \quad (3)$$

what places the deviatoric state along the diagonal (normal stresses), where the hydrostatic state is subtracted, remaining the nonhydrostatic state.

For an isotropic, linear elastic, medium, the relation between stress and strain is represented by Hooke's law: $\sigma_{ij} = \lambda\theta\delta_{ij} + 2\mu\varepsilon_{ij}$, where λ and μ are the Lamè elastic parameters, and δ_{ij} the Kronecker delta ($\delta_{ij} = 0$, if $i \neq j$ and $\delta_{ij} = 1$, if $i = j$). The nondimensional parameter θ represents the cubic dilation, and is given by the divergence of the displacement vector $\vec{u}$ as: $\theta = \nabla \cdot \vec{u} = \frac{\partial u_x}{\partial x} + \frac{\partial u_y}{\partial y} + \frac{\partial u_z}{\partial z}$.

The nondimensional tensor components ε_{ij} are defined in terms the displacement components u_i in the form: $\varepsilon_{ij} = \frac{1}{2}\left(\frac{\partial u_i}{\partial x_j} + \frac{\partial u_j}{\partial x_i}\right)$. Besides that, the linear shear-extensional tensor, an nondimensional rotation tensor is also expressed as: $\varphi_{ij} = \frac{1}{2}\left(\frac{\partial u_i}{\partial x_j} - \frac{\partial u_j}{\partial x_i}\right)$.

Governing equations

Since this phenomenon is also related to elastic wave propagation, the system equations of motion are resumed to the form: $\frac{\partial \sigma_{ij}}{\partial x_j} = \rho\frac{\partial^2 u_i}{\partial t^2}$, $(i,j = 1,2,3)$, or $(i,j = x,y,z)$. This means that the spatial stress variation is related to the inertial forces (per unit volume), not considering internal forces in this case. The basic seismic velocities (P and S) for elastic, homogeneous, isotropic media are given by: $v_P = \sqrt{(\lambda + 2\mu)/\rho}$, $v_S = \sqrt{\mu/\rho}$, where μ is the shear module, ρ is the volumetric density, and λ is related to the bulk and shear modules. From the above relations, the shear module is calculated by: $\mu = v_S^2\rho$, $\lambda = v_P^2\rho - 2\mu = (v_P^2 - 2v_S^2)\rho$, and the ratio $\gamma = v_S/v_P$.

Density is usually admitted as a parameter that varies slowly with depth, from the earth's surface to the top of the target interface; but, in some geological situations the density discontinuity may be relatively high. In the present case, the density is modeled in 2D, $\rho = \rho(x,z)$, and is integrated in the calculation grid.

The system of differential equations to be integrated, that corresponds to the description of the static problem, has the null time variation, governing a part (layer) of the medium, which is summarized to the form: $\frac{\partial \sigma_{1j}}{\partial x_j} = \rho g\delta_{3j}$. This means that the sum for the horizontal stress variations are zero, and for the vertical component is controlled by the gravitational load of the subsurface expressed in terms of force per unit area (ρg). Therefore, the lateral tectonic stresses are not taken into account in this model. Also, in other cases the quantities ρ and g can be considered as spatial functions; that is, $\rho = \rho(x,y,z)$ and $g = g(x,y,z)$.

We describe as a first medium model that formed by plane-horizontal layers. The equilibrium equation for the linear elastic medium for each layer is given by: $\frac{\partial \sigma_{ik}}{\partial x_k} = \rho g_i$, where σ_{ik} represents the components of the stress tensor, ρ the rock density, and g_i the gravity acceleration. For the case of vertical gravity, $g_{i=z}(z) \approx g$, admitted as constant for a small depth variation, is simplified to the form: $\frac{\partial \sigma_{zz}}{\partial x_z} = \rho g$. This equation has an elementary solution that is given by: $\sigma_{zz}|_{z=z_0} = \int_{z=0}^{z=z_0} \rho g dz = \rho g z_0 = P_0(z_0)$, where $P_0 = \rho g z_0$ is the overload rock weight per unit area; i.e., the vertical pressure due to the overload at any depth z_0.

For the present model, the vertical stress, $\sigma_{zz}(z)$, is defined as equal to overloading layer; i. e., $\sigma_{zz} = P_z = P_0(z)$. The horizontal stress, $\sigma_{xx}(z)$, considering that $\sigma_{yy} = \sigma_{xx}$, is smaller than vertical stress, σ_{zz}, and is demonstrated to be given by $\sigma_{xx} = P_x = P_0(1 - 2\gamma^2)$, where $P_0 = P_0(z)$, $\gamma = \gamma(z) = v_S(z)/v_P(z)$.

The scalar invariant hydrostatic pressure field, $P(z) = P_H$, was defined above as the average $P = P_H = \frac{1}{3}(\sigma_{xx} + \sigma_{yy} + \sigma_{zz})$. Using Hooke's generalized law, it is demonstrated to be given by $P = P_H = (\lambda + \frac{2}{3}\mu)\theta$, where $\theta(z)$ is the cubic dilation, and $\lambda(z)$ and $\mu(z)$ are Lamè's parameters described before.

Another important physical feature is the pressure discontinuity at the interfaces between layers ($\Delta P = P^+ - P^-$), at the depth z (positive down), which exists if the speed ratio γ exhibits a discontinuity. Considering the case of a medium formed by plane-horizontal layers, and Hooke's law, it is shown that the discontinuity ΔP is given by $\Delta P(z) = \frac{4}{3}(\gamma_1^2 - \gamma_2^2)P_0(z)$, where γ_1 is the upper layer and γ_2 the lower layer parameter, across the interface positioned at the depth z, and the overload pressure varies by positive and negative jumps. This idea may seem a little strange in simple geological descriptions, but it is a fact related to the non-elementary behavior of stress in solids.

The intensity of tangential stress is a way of measuring the mechanical instability responsible for the ability to destroy the granular structure and produce fracture of the solid rock, and the following result is obtained: $P_T = \frac{1}{2}(\sigma_{zz} - \sigma_{xx}) = \gamma^2 P_z$, and again the above result also depends on the γ ratio.

RESULTS

The velocities were obtained based on controlled empirical models with the parameters presented in the Table 1, where A1 represents the water layer (dark blue), A2 a layer overlying the reservoir (light blue), A3 the reservoir (yellow), A4 the layer that includes the generator (red), and A5 the basement (brown).

Table 1: Example of used parameters.

Valor	A1	A2	A3	A4	A5
γ_0	0	0.687	0.807	0.677	0.570
v_{P0}	1500	2280	3442	4222	5002
k_P	0	1.5	0.5	0.75	0.5
k_g	0.0001	0.0001	0.0001	0.0001	0.0001

The formula for the velocity v_P was given by $v_P = v_{P0} + k_P z$, for the $\gamma = \gamma_0 + k_g z$, and for the density as $\rho = 0.452 + 0.4788 v_P$.

The basic sections for the pressure prediction are the velocity v_P and the ratio γ, from where the others are calculated (Figures 2, 3 and 4). In order to obtain these two sections, we started from the CRS stack interpreted sections, where the generator and reservoir formations were selected based on geological information.

The empirical v_P models are mixed, and composed of jumps and smooth linear variation; thus, for the solid formations a vertical gradient was assigned to the P wave velocity in the form $v(n) = v_0 + kn$ (in the experiment k varied between 0.1 and 0.7) , where $z = 1$ was admitted. The empirical model for the γ ratio was represented only by jumps. From the v_P and γ information, the distribution for v_S was calculated. Figure 5 shows the density distribution, ρ, of the example, which also followed the mixed pattern similar to those for v_P; that is, with jumps and smooth vertical gradient.

The vertical pressure figures, $P_z = \sigma_{zz} = P_0$, show a very smooth behavior as expected, and for the sake of space are not presented here. Now, the figures 6 for the horizontal pressure, $P_x = \sigma_{xx} = P_0(1 - 2\gamma^2)$, show a very differentiated and special behavior in each section. The figures 7 of the deviatoric pressure between vertical and horizontal pressures, $P_T = \frac{1}{2}(\sigma_{zz} - \sigma_{xx})$, show a very special behavior for the low and high zones, and whether positive or negative, and the information is that the vertical exceeds the horizontal pressure.

The hydrostatic pressure (solid) figures 8, $P_H = \frac{1}{2}(\sigma_{xx} + \sigma_{zz})$, clearly model the low pressure zone (central blue stripe) between two high pressure zones (weaker above and stronger below). But it is interesting that part of the basement presents zones of intermediate pressure.

The figures of the pressure jump, $\Delta P(z) = \frac{4}{3}(\gamma_1^2 - \gamma_2^2)P_0(z)$ (γ_1 is above and γ_2 below the separating interface), expose faint lines of the discontinuities that serve to mark the different formations, and the quality of the process, but they were not presented here due to to space. Similarly, the figures of the Poisson's coefficient, $\nu = \frac{\Delta x}{\Delta z}$, clearly model, in some detail, negative values for the low pressure zone, and smooth gradients for the other formations, and positive values.

Figure 2: Velocity v_P.

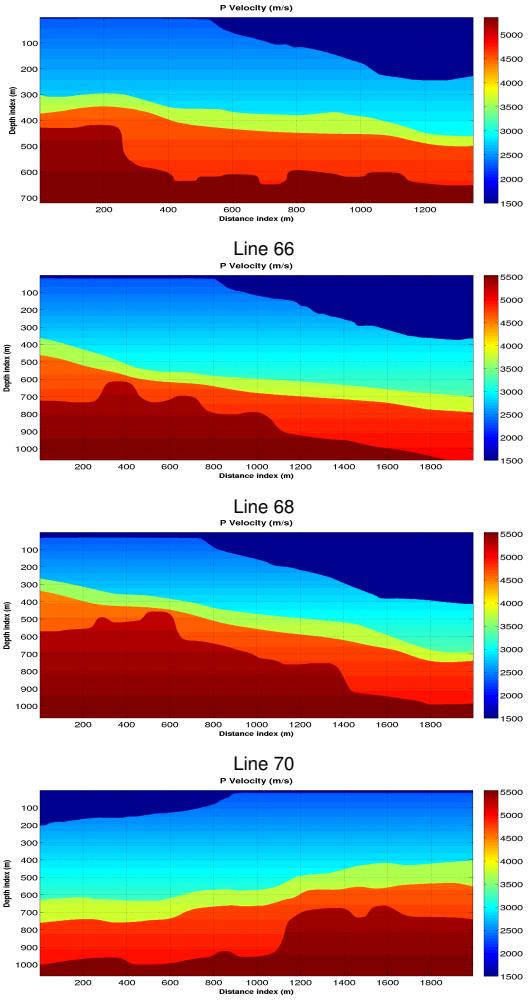

Conclusions

The seismic data were processed with CRS technology, which proved to be more effective in the geometrical delineation of reflectors of the stacked and migrated

Figure 3: Gamma Ratio.

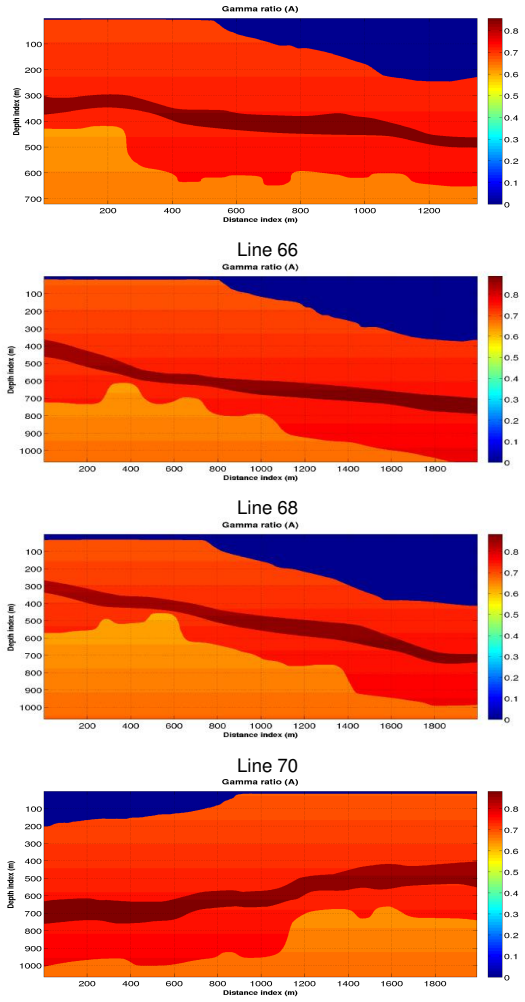

Figure 4: Velocity v_S.

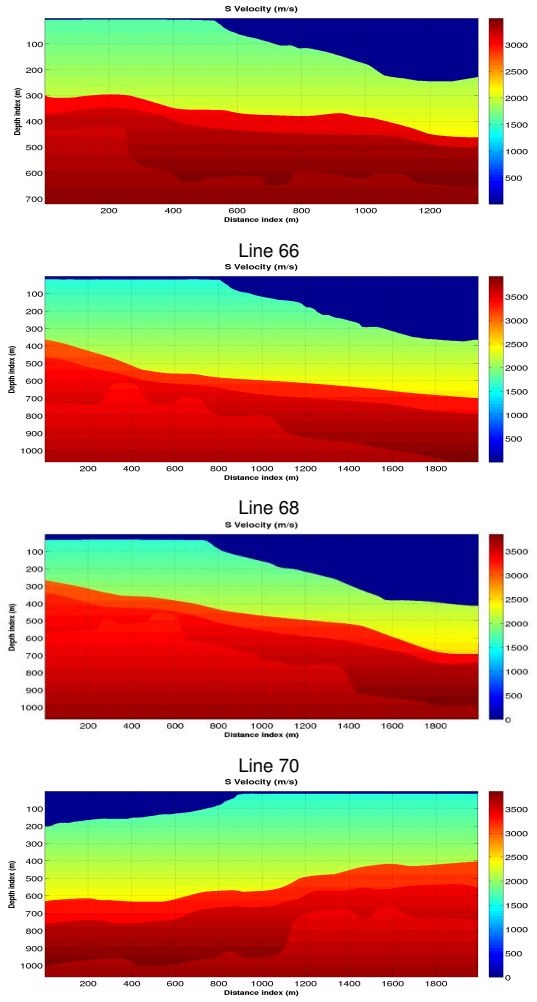

sections, that was used to construct an empirical velocity and density model.

The mapping of a low pressure zones, corresponding to a proposed reservoir rock, has a spatial extension that depends on the seismo-stratigraphic and structural interpretation.

A deeper continuation of this work requires borehole, structural, and tectonic information for the area; but this type of information has limits to public use due to property contracts.

References

Cohen, J. K., and Stockwell, J. J. W., 2005, Cwp/su: Center for Wave Phenomena, Colorado School of Mines.

Mann, J., 2002, Extensions and aplications of the common reflection surface stack method: Ph.D. thesis, Karlsruhe University, Karlsruhe.

Mello, M. R., Gonçalves, F. T. T., and Telnaes Netto, A. S., 1994, A successful application of the petroleum system concept in the camamu basin offshore brasil.: In: FIRST POINT AAPG/AMPG RESEARCH CONFERENCE GEOLOGICAL ASPECTS OF PETROLEUM SYSTEMS.

Payton, C. E., 1977, *(Ed).* seismic stratigraphy - applications to hydrocarbon exploration: American Association of Petroleum Geologists. (Memoir, 26), Tulsa, OK.

Persen, L. N., 1975, Rock dynamics and geophysical exploration: Elsevier Scientific Publishing Company, Amsterdam, Holland.

Sibiryakov, E. P., Leite, L. W. B., and Vieira, W. W. S., 2014, Model of the structured continuum, and the relation between specific surface area, porosity and permeability: Brazilian Journal of Geophysics, **31**, no. 4, 559–568.

Sibiryakov, E. P., Leite, L. W. B., and Vieira, W. W. S., 2015, Behavior of stresses in structures and the effect on hydrodynamics analyzed from multicomponent seismic data: Brazilian Journal of Geophysics, **33**, no. 1, 57–70.

Silva, A. N. P., 2016, Processamento, imageamento e cálculo de predição de pressão de dados sísmicos numa

Figure 5: Density.

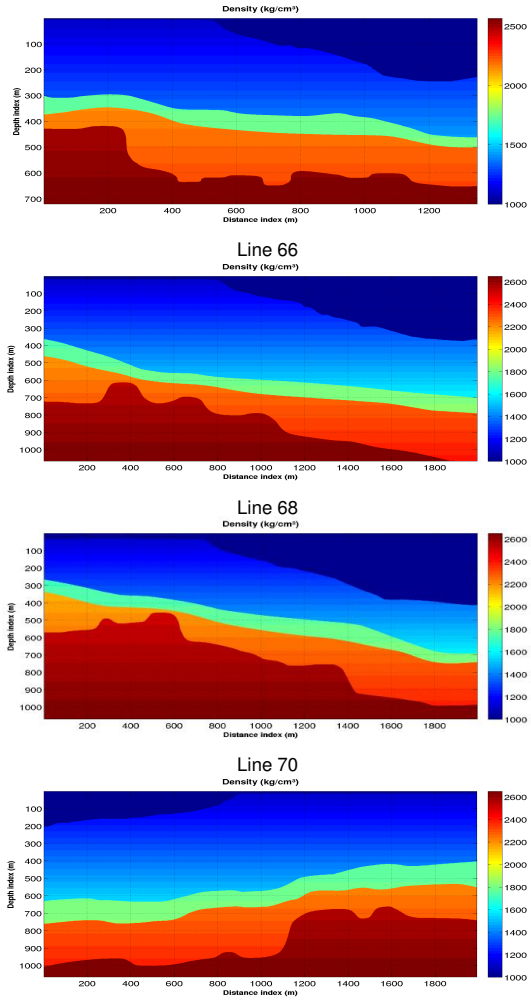

bacia sedimentar: Master's thesis, UFPA, Belém, Pará, Brazil.

Acknowledgments

The authors would like to thank the sponsorship of Project INCT-GP, and also in special to the Project PRH-06, that are present in part of this research work. We extend our thanks also to CAPES and CNPQ for the scholarships.

Figure 6: P_x.

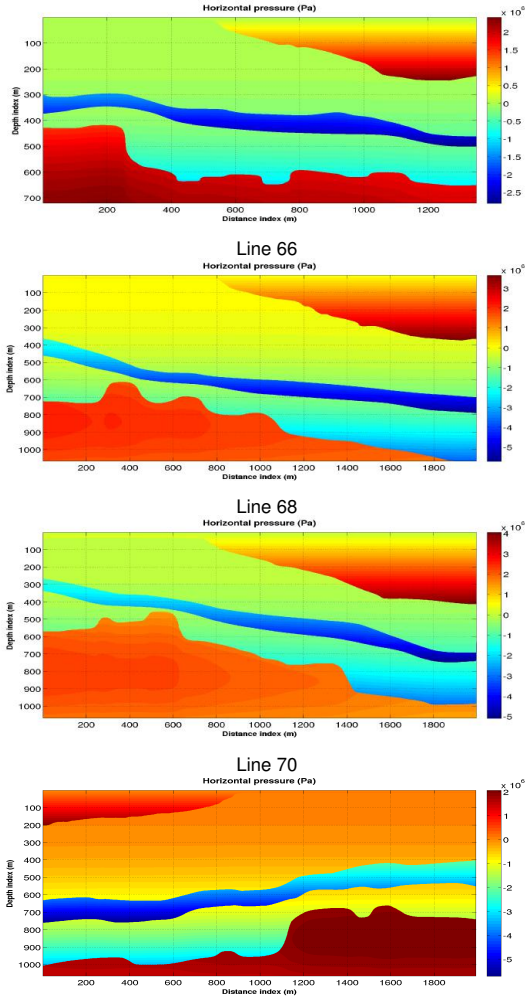

Figure 7: P_T.

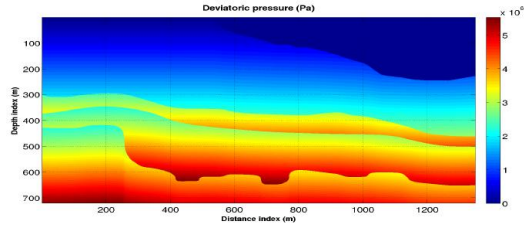

Line 66

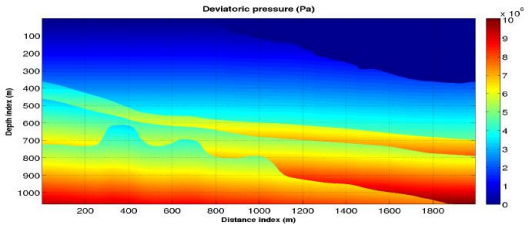

Line 68

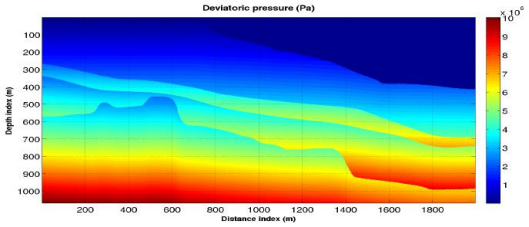

Line 70

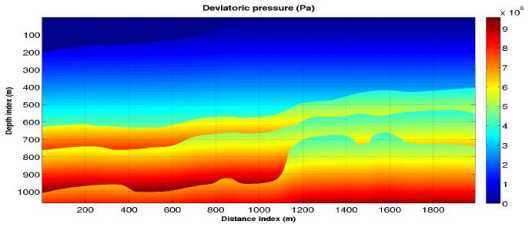

Line 97

Figure 8: P_H.

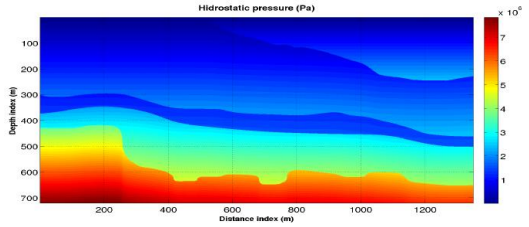

Line 66

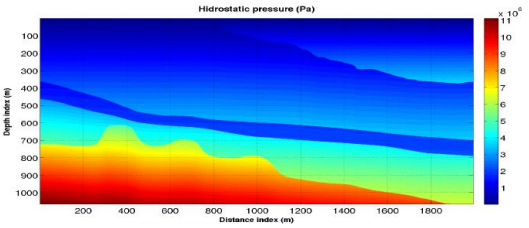

Line 68

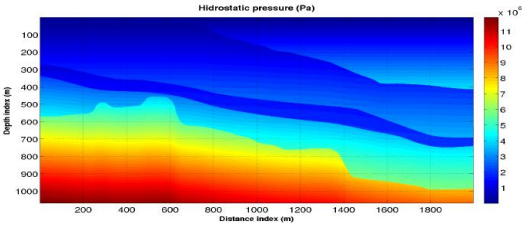

Line 70

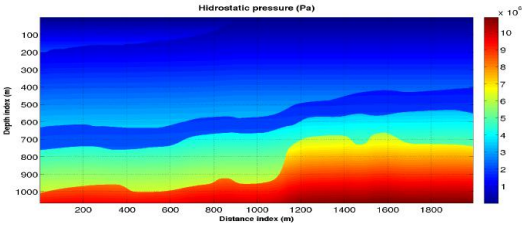

Line 97